Turkish Journal of Earth Sciences

Volume 32
Number 3 *SI-3*

Article 11

1-1-2023

Paleoseismology of the Sürgü and Çardak faults - splays of the Eastern Anatolian Fault Zone, Türkiye

MUSA BALKAYA

HÜSNÜ SERDAR AKYÜZ

SÜHA ÖZDEN

TÜBİTAK

Turkish Journal of Earth Sciences

http://journals.tubitak.gov.tr/earth/

Research Article

Turkish J Earth Sci
(2023) 32: 402-420

doi:10.55730/1300-0985.1851

Paleoseismology of the Sürgü and Çardak faults—splays of the Eastern Anatolian Fault Zone, Türkiye

Musa BALKAYA[1,*], Hüsnü Serdar AKYÜZ[2], Süha ÖZDEN[3]

[1]Department of Construction, Vocational School of Technical Sciences, Kahramanmaraş Sütçü İmam University, Kahramanmaraş, Türkiye

[2]Department of Geological Engineering, Faculty of Mines, İstanbul Technical University, İstanbul, Türkiye

[3]Department of Geological Engineering, Faculty of Engineering, Çanakkale Onsekiz Mart University, Çanakkale, Türkiye

Received: 18.04.2022 • **Accepted/Published Online:** 11.04.2023 • **Final Version:** 28.04.2023

Abstract: The sinistral East Anatolian Fault Zone (EAFZ) and the dextral North Anatolian Fault Zone (NAFZ) are two important strike-slip faults that delimit the boundaries of the Anatolian plate. The north-south directed compressional forces in eastern Türkiye trigger the westward escape of the Anatolian plate along these prominent structures. This study aims to reveal the earthquake history of the Sürgü and Çardak faults, which are important fault segments that splay from the EAFZ. In this context, overall, four paleoseismologic trenches were dug, two trenches on the Sürgü Fault and two trenches on the Çardak Fault. Along the Sürgü Fault, at least two paleoearthquake events have been determined on the trench walls, one event occurred around 3400 BCE and the second event happened between 2085 ± 65 BCE and 790 ± 20 BCE. Moreover, trenching results from the Çardak Fault indicate two surface rupturing paleoearthquakes between 10520 ± 95 BCE and 5780 ± 65 BCE, and between 3215 ± 125 BCE and 825 ± 55 CE, respectively. The focal mechanisms of important instrumental earthquakes around the Sürgü and Çardak faults on the EAFZ show that NNE-SSW trending compressional forces are actively dominating the tectonic setting of the region in the contemporary era. Paleoseismological investigations suggested that the Sürgü and Çardak faults have the potential to produce surface-rupturing earthquakes with an estimated magnitude of 7 or larger.

Key words: SE Türkiye, East Anatolian Fault Zone, earthquake, paleoseismology

1. Introduction

The Eastern Anatolia Region forms the continent-continent collision area of the Eurasian and Arabian/African plates (Dewey et al, 1986). As a result of this collision that started in the Late Miocene, the Anatolian block started to escape to the west along the dextral North Anatolian Fault Zone (NAFZ) in the north and the sinistral East Anatolian Fault Zone (EAFZ) in the south (Figure 1a; Şengör and Yılmaz, 1981; Barka and Reilinger, 1997). These two strike-slip fault zones are highly active structural elements and have shaped the morphology with major earthquakes for millions of years. The EAFZ consists of many segments (Allen, 1969; Arpat and Şaroğlu, 1975; Şaroğlu et al., 1992; Emre et al., 2013). In addition to its segments along its extension, it also has splay faults, including the Sürgü and Çardak faults, extending westward into the Anatolian block starting from the south of Çelikhan. There is a debate on the kinematics of these faults. Several studies stated that these two faults, which are approximately 160-km long, synthetic offshoots of the EAFZ (Arpat and Şaroğlu, 1975; Perinçek and Kozlu, 1984; Perinçek et al., 1987; Yılmaz, 2002; Westaway, 2004; Yılmaz et al., 2006; Emre et al., 2016; Balkaya et al., 2021; Balkaya, 2022; Güvercin et al., 2022) and defined as the northern strands of the EAFZ (Duman and Emre, 2013). In some studies, it is suggested that the Sürgü Fault is a right-lateral strike-slip fault (Koç, 2005; Sunkar et al., 2008; Koç and Kaymakçı, 2013; Gülerce et al., 2017). Sürgü and Çardak faults run through many settlements such as Çelikhan, Kurucaova, Sürgü, Nurhak, Barış, Ekinözü, Çardak, Göksun. There exist many geological, geomorphological and neotectonic studies on this segment in the literature (Perinçek and Kozlu, 1984; Perinçek et al., 1987; Yılmaz, 2002; Westaway, 2004; Koç, 2005; Sunkar et al., 2008; Duman and Emre, 2013; Koç and Kaymakçı, 2013; Emre et al., 2016). However, the earthquake history of these faults is obscure. Although earthquakes affecting the region are mentioned in the historical records, there is no information about which faults these earthquakes are related to. There are no paleoseismological trench studies and dated earthquakes associated with these faults in the region (Figure 1b). Paleoseismological data

* Correspondence: musabalkaya@ksu.edu.tr

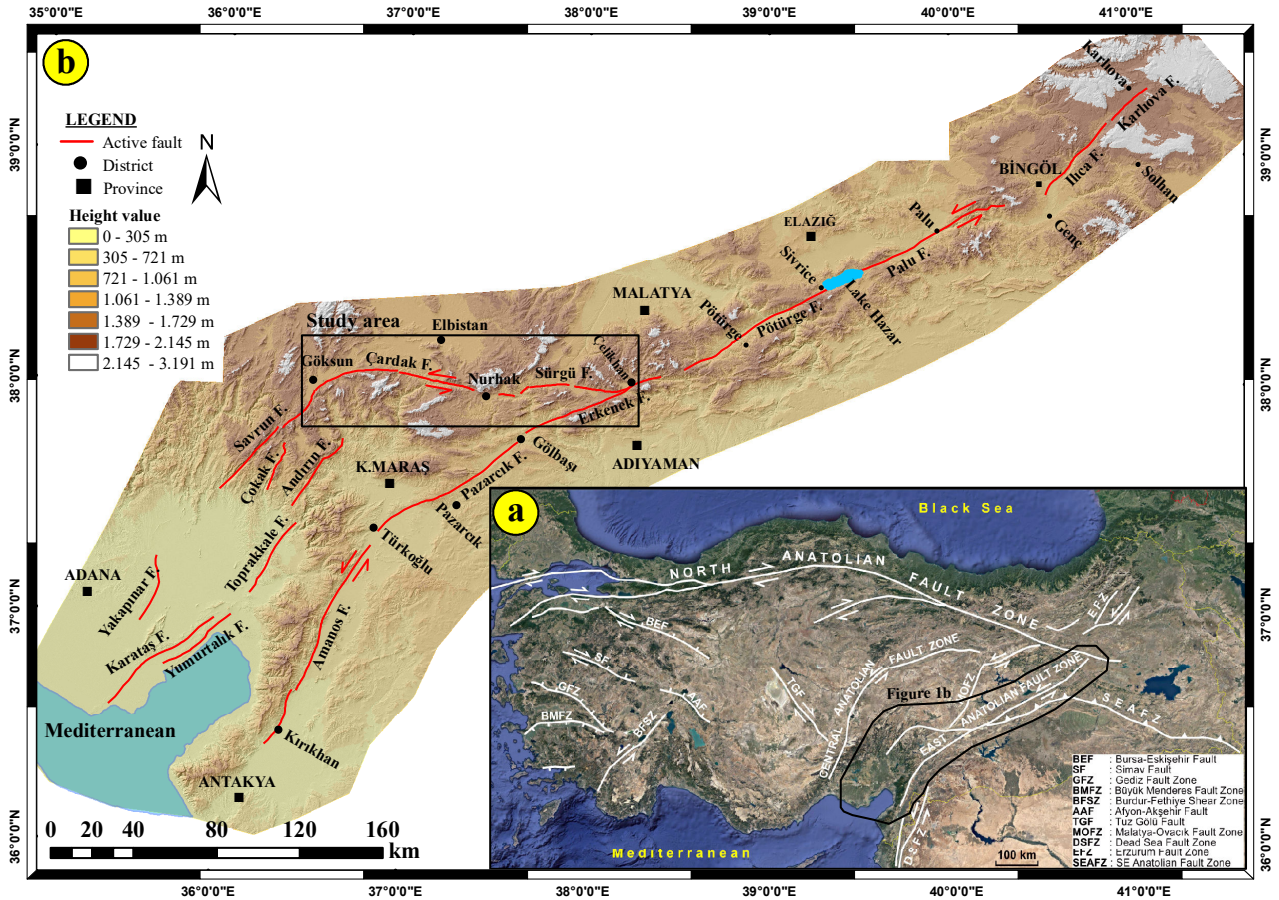

Figure 1. (a) Location of the EAFZ on an active fault map of Türkiye. (b) The geometry and segmentation of the EAFZ and location of the study area (simplified from Duman and Emre (2013)).

from Sürgü and Çardak faults are first presented with this study. The approximate dates of surface rupture producing earthquakes and the timing of the latest earthquake on the Sürgü and Çardak faults were determined and evaluated together with current seismological data. There has been no major earthquake that caused surface ruptures for a long time on the Sürgü and Çardak faults (about last 500 years according to Duman and Emre (2013)); thereby, revealing the earthquake hazard potential of these faults, is of utmost importance in terms of industrial and civil projects, and especially life safety in this region.

2. Geological and tectonic setting

A geological map of an approximately 160-km long and 15-km wide area (with nearly E-W direction) that covers the Sürgü and Çardak faults was compiled (Figure 2). Through the preparation stages of the geological map, 1/100,000 scaled geological map sheets prepared and published by the General Directorate of Mineral Exploration and Research (MTA) were utilized (Bedi and Yusufoğlu, 2018; Çoban and Dalkılıç, 2018; Sümengen, 2014a and 2014b; Usta et al., 2018). Lithological units in the study area are divided into 3 groups: the pre-Miocene basement rocks, Miocene units, and post-Miocene units. The pre-Miocene basement rocks, which are dominant across the study area, contain different igneous, metamorphic and sedimentary rock types (Bedi and Yusufoğlu, 2018; Çoban and Dalkılıç, 2018; Sümengen, 2014a and 2014b; Usta et al., 2018). Miocene units are widespread in the southern parts of the Çardak Fault. The post-Miocene units in the study area are divided into two groups: first, Plio-Quaternary units, and second, Quaternary units. The Plio-Quaternary units are dominant around Kurucaova in the southeast of the Sürgü Fault, in the north and northwest of the Sürgü Fault, and in the north of the Çardak Fault. Quaternary units consisting of alluvium, colluvium, old and young alluvial fan deposits are observed along the valleys and basins that are cut by faults (Figure 2). Based on the results of the field and office studies, and by considering the lithological, structural, and geomorphological features of the study area, the Sürgü and Çardak faults were mapped. Other active faults and folds in the study area were also added to the geological map

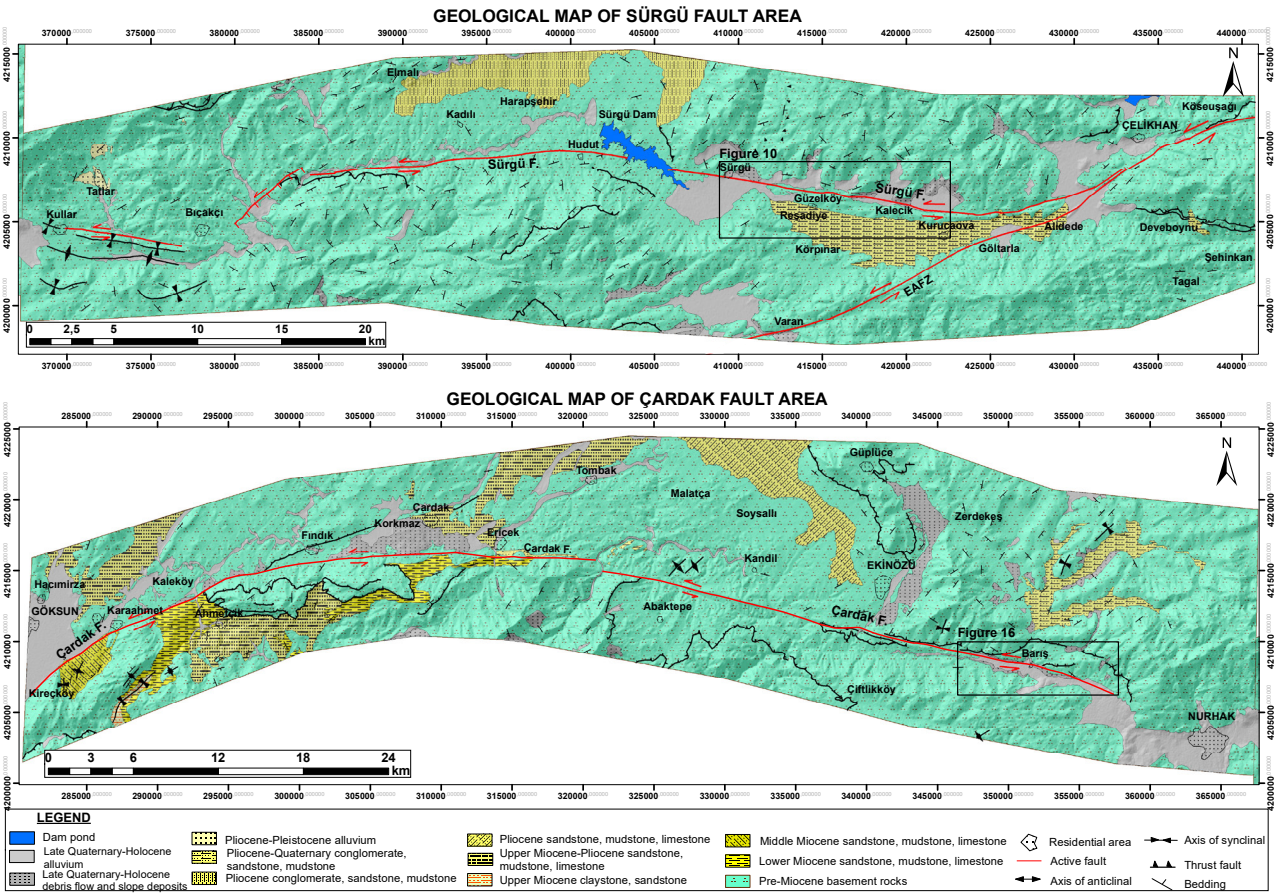

Figure 2. Simplified geological map of the study area (compiled from 1/100,000 scale sheets of MTA geology database (Bedi and Yusufoğlu, 2018; Çoban and Dalkılıç, 2018; Sümengen, 2014a and 2014b; Usta et al., 2018)).

based on the current active fault map of Türkiye (Emre et al., 2013; Figure 2).

2.1. East Anatolian Fault Zone

The EAFZ is a 580-km long left-lateral strike-slip fault zone and first proposed and named by Arpat and Şaroğlu (1972). Researchers also published first fault map of the EAFZ (Arpat and Şaroğlu, 1975). This fault zone starts from Karlıova in the northeast, runs through Kahramanmaraş, and ends at the Dead Sea Fault. Its main strand between Karlıova and Antakya is divided into 7 fault segments by Emre et al. (2016). These are namely: Karlıova, Ilıca, Palu, Pötürge, Erkenek, Pazarcık and Amanos segments (Figure 1b). A fault strand that diverges to the west in the south of Çelikhan was named as the northern segment of the EAFZ by Duman and Emre (2013). The fault segments on this branch are named as Sürgü, Çardak, Savrun, Çokak, Yakapınar, Andırın, Toprakkale, Yumurtalık and Karataş fault segments (Figure 1b; Duman and Emre, 2013; Emre et al., 2016). The same nomenclature is used for the segments that are referred in this study.

Although the onset age of the EAFZ is controversial, a Late Pliocene age is widely accepted among researchers (Şaroğlu et al., 1987; Westaway, 2004; Yönlü et al., 2013). According to GPS (Global Position System) data, the slip rate of the fault zone is approximately 10 mm/year (McClusky et al., 2000; Reilinger et al., 2006). According to the geological data, the slip rate ranges between 4 mm/year and 11 mm/year (Herece, 2008; Yönlü et al., 2013; Emre et al., 2016). Duman and Emre (2013) suggested that, based on the systematic offsets along the Holocene drainage networks, the faults denote slip rates of 3 mm/year on Sürgü Fault and 2.5 mm/year on Çardak Fault.

Left lateral Sürgü and Çardak faults are separated from each other with Nurhak Fault Complex (Duman and Emre, 2013), a compressional structure due to right-stepping between fault branches (Figure 1b). Therefore, these two faults were evaluated separately.

2.2. Sürgü Fault

The Sürgü Fault splays from the EAFZ at the south of Çelikhan and ends at the east of Nurhak (Figure 1b).

The Sürgü Fault is an active sinistral strike-slip fault that extends for about 70-km in the E-W direction (Perinçek and Kozlu, 1984; Perinçek et al., 1987; Yılmaz, 2002; Westaway, 2004; Korkmaz et al., 2008; Duman and Emre, 2013; Emre et al., 2016; Balkaya et al., 2021). Yılmaz (2002) stated that on the Sürgü Fault, to the west of Kurucaova, a cumulative 4-km left lateral offset was detected at the lithological boundaries. Although the eastern section of the Sürgü Fault up to Sürgü is dipping to the north, the western section of the Sürgü is dipping to the south with an angle of 85° and this dip angle decreases towards the deeper parts (Taymaz et al., 1991; Yılmaz, 2002). In the study conducted by Koç and Kaymakçı (2013) on the Sürgü Fault, it was claimed that the western part of the fault is mainly controlled by dextral strike-slip motion with a reverse component, yet the eastern part has a normal component. Duman and Emre (2013), on the other hand, stated that a Holocene aged alluvial fan was offset left-laterally along the Sürgü Fault.

In this study, Sürgü Fault was divided into four segments by considering the geometrical characteristics of the fault (Figure 3a). The 50-km long section of the fault that starts in the south of Çelikhan and passes through Sürgü village and ends in Küçüklü village runs in the east-west direction. The eastern section of the Sürgü Fault, from the NE of Kurucaova to the east of Sürgü, extends through the north of a linear ridge (Figure 4). On the wall of a road cut in the Sürgü village, it has been observed that the Late Quaternary colluvium and alluvium deposits are cut by the Sürgü Fault (Figure 5). In this place, the attitude of the fault is measured as 280/78 NE.

The Sürgü Fault makes a 4-km-step to the left at the west of Küçüklü village (Figure 3a). After this step, which is characterized by normal faulting and local extension,

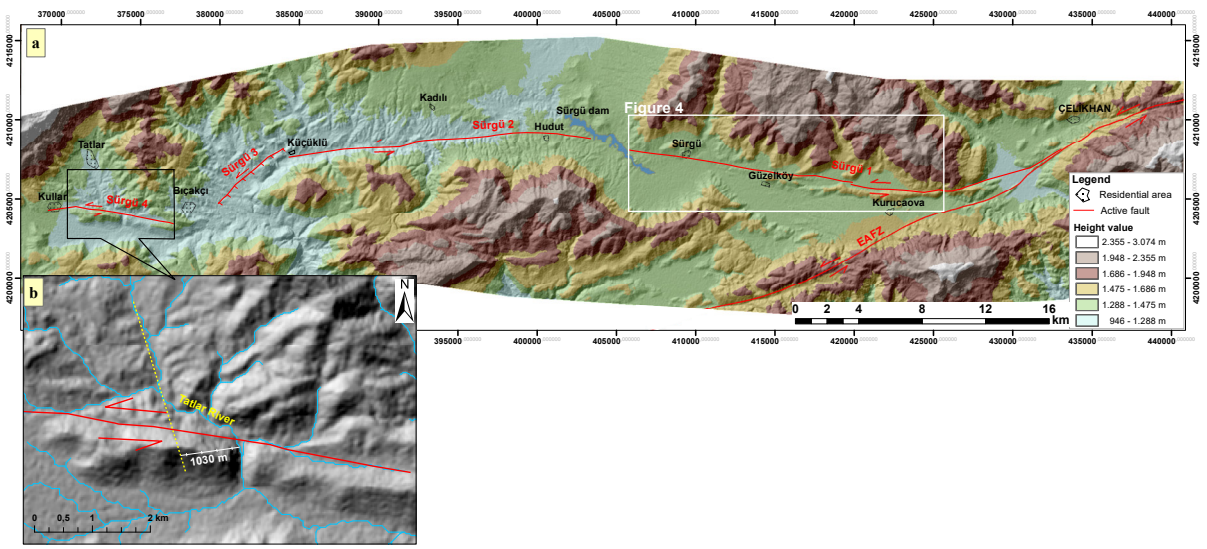

Figure 3. a) Physiography of the Sürgü Fault and its segmentation into four sections (Sürgü-1 to -4), b) the sinistral offset of Tatlar creek on DEM.

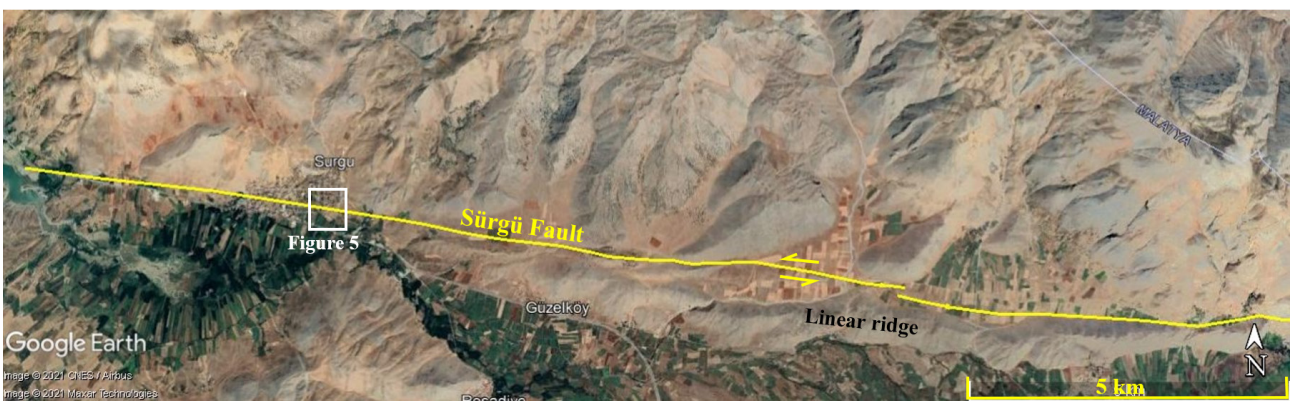

Figure 4. The Sürgü Fault between Kurucaova and Sürgü Dam.

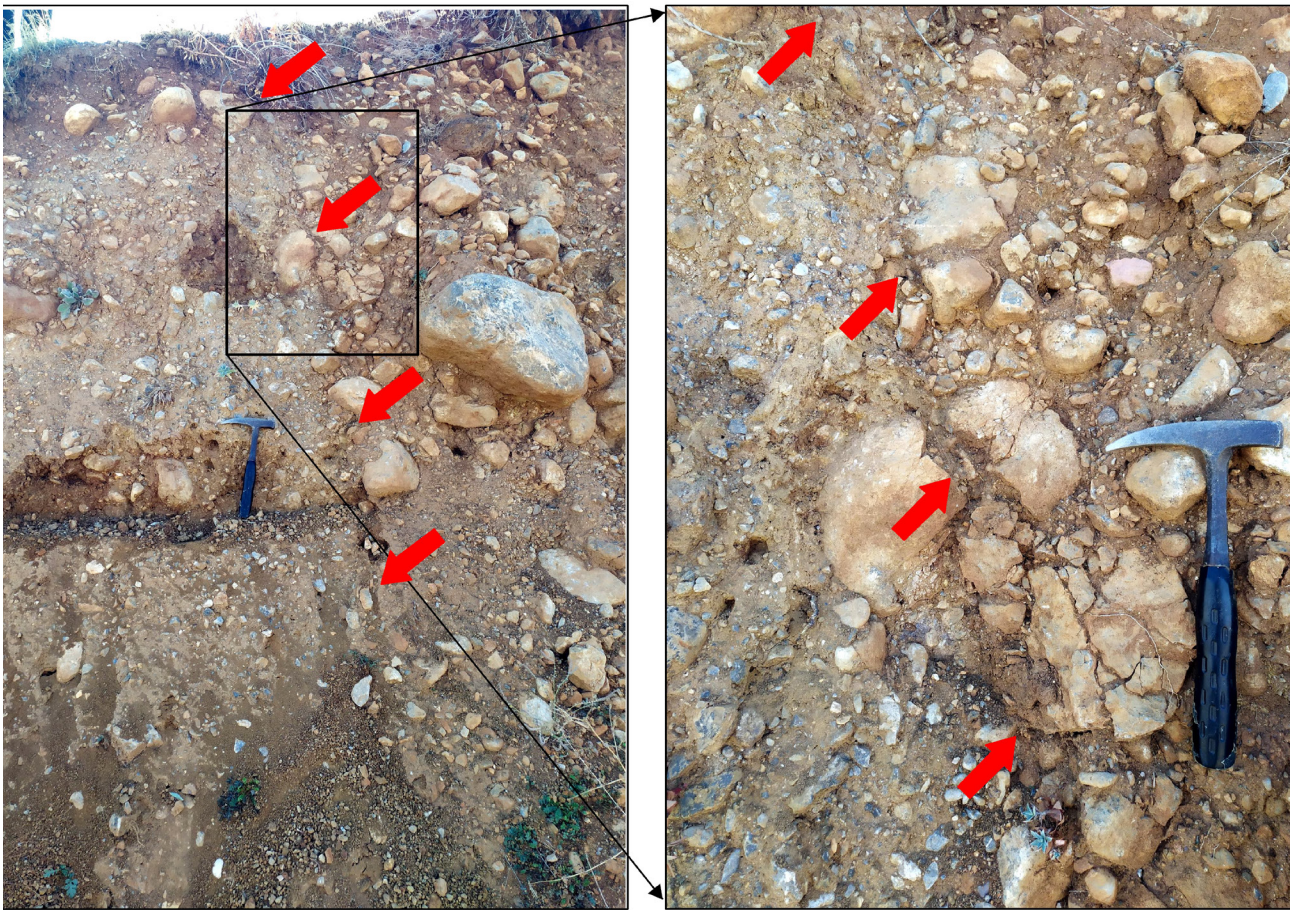

Figure 5. The Sürgü Fault in exposure, cutting Late Quaternary deposits in Sürgü district (view to west).

the fault runs again in the E-W direction toward Nurhak (Figure 3a). Structural and morphological elements such as stream and river offsets, linear troughs, and shutter ridges were determined in various places along the Sürgü Fault with the help of field studies, the Google Earth program, and plotted drainage network systems on the digital elevation model (DEM; see Balkaya (2022) for details). In particular, 9-km east of Nurhak town, on the DEM and the Google Earth images, it is clearly observed that Tatlar creek is sinistrally offset about 1-km by the Sürgü Fault (Figure 3b).

2.3. Çardak Fault

The length of the Çardak Fault is approximately 80-km and it is located between Nurhak and Göksun (Figure 6). In the west of Nurhak, the fault extends to the west with an N80°W orientation; then continuing within a narrow deformation zone, the fault runs to the south of Göksun with a concave geometry. Duman and Emre (2013) indicated that the 50-km long western part of the Çardak Fault cuts the old thrusts and folds and represents an active left-lateral fault morphology, moreover the Holocene river valleys were offset sinistrally by the fault.

In this study, the Çardak Fault is considered as two separate segments and named: Çardak-1 and Çardak-2 (Figure 6). The Çardak-1 segment, which forms the 37-km long eastern part of the Çardak Fault, starts in Nurhak and extends westward through Barış village and south of Ekinözü and reaches the SE of Karadut. In the south of Karadut, the Çardak Fault steps 700 m to the right (Figure 6). The 43-km long Çardak-2 segment starts from the south of Karadut and runs to the south of Çardak and ends to the south of Göksun.

Structural and morphological elements such as offset streams, fault scarps, small depression basins, linear valley floor, and linear troughs were determined in various places along the Çardak Fault. On the Google Earth images and during field studies it is clearly observed that alluvial deposits in a stream that runs through Barış village, where the eastern section of the Çardak Fault extends, is offset sinistrally 70 m by the fault (Figures 7 and 8). It is observed that basement units (serpentinite) crop out just below the Late Quaternary deposits in the northern block of the fault here. Additionally, abrupt topographic elevation differences (fault scarp) were also observed around Barış

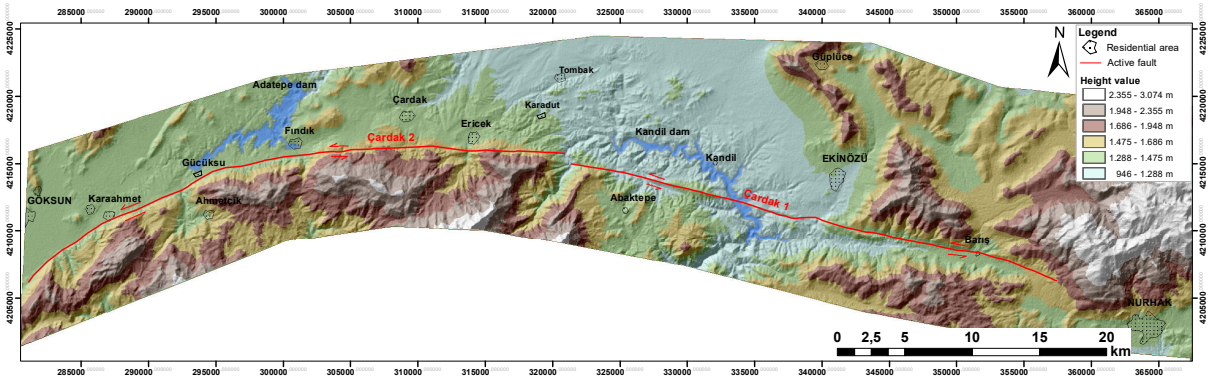

Figure 6. Physiography of the Çardak Fault segmented into two sections.

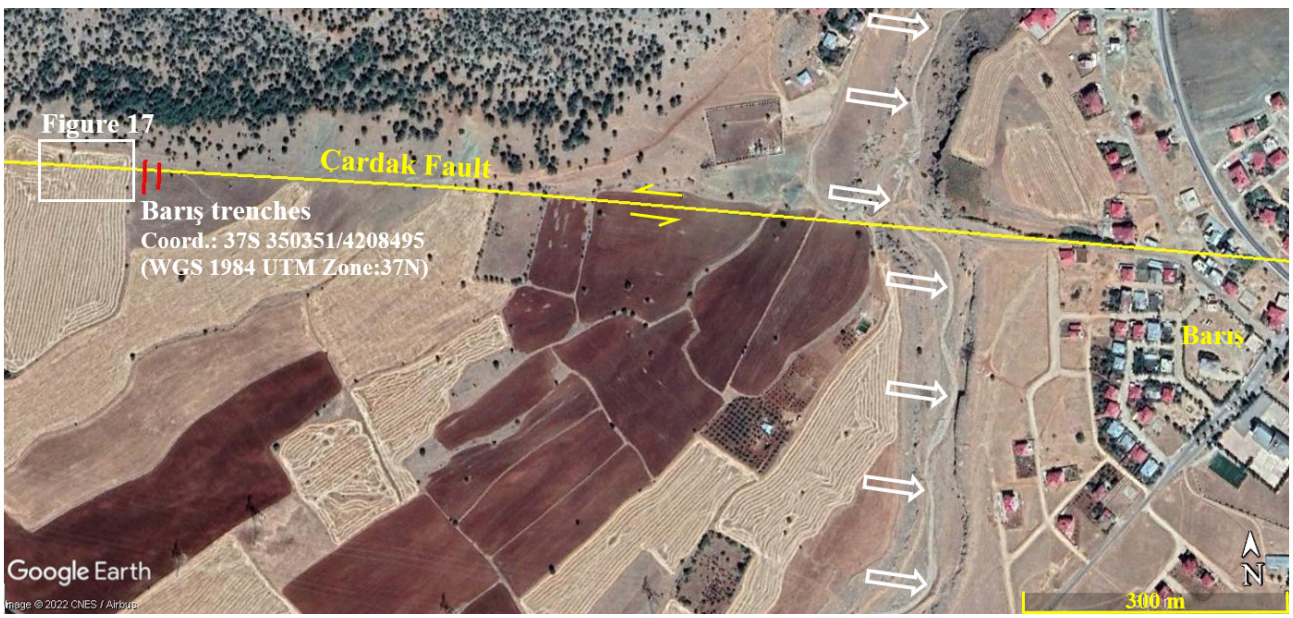

Figure 7. Google Earth image showing the 70-m stream offset through Barış village. White arrows indicate the sinistral deflection emphasized by the stream bed.

village, which indicates that the southern block moved downward along an east-west orientated fault trace (Figure 8).

3. Macroseismicity

According to historical and instrumental earthquake records, many earthquakes have occurred in the vicinity of the Sürgü and Çardak faults (Taymaz et al., 1991; Guidoboni et al., 1994; Guidoboni and Comastri, 2005; Ambraseys, 2009; Duman and Emre, 2013). Based on historical earthquake records, the Arabissus (current Elbistan/Kahramanmaraş) settlement, which was founded by Byzantine emperor Maurice, was destroyed twice by two major earthquakes in CE 584/585 and CE 587 (Guidoboni et al., 1994; Ambraseys, 2009). It is stated that the 584/585 Arabissus earthquake occurred with an intensity of IX-X (Guidoboni et al., 1994). Considering the location of Elbistan (see Balkaya (2022) for map and details, pages 70–71) and the neighboring active faults, it is likely that at least one of the earthquakes was generated by the Çardak Fault.

From seismic records in the instrumental period, two damaging earthquakes occurred around Doğanşehir in the north of the Sürgü Fault in 5 May (M = 5.8) and 6 June (M = 5.6) 1986 (Taymaz et al., 1991; Yılmaz, 2002; Duman and Emre, 2013). Further macroseismic instrumental data for the Çardak Fault is as follows. Seismic data obtained from Boğaziçi University Kandilli Observatory and Earthquake Research Institute National Earthquake Monitoring Center

(KOERI-RETMC, 2021)[1] indicates earthquakes with a magnitude of 5.5, 5.0, and 4.2 occurred in the southwest of Ekinözü in 1922, in the vicinity of Nurhak in 1978, and in the vicinity of Ortaören (Ekinözü) in 2013, respectively (Figure 9).

The strike, dip, and rake angles of the 1986 Doğanşehir earthquakes and the 2013 Ekinözü earthquake are collected from various sources (Taymaz et al., 1991; Tan et al., 2008; Ekström et al., 2012; Global CMT, 2021[2]; AFAD, 2021[3]) and represented in Table 1. Based on this data, the focal mechanism inversions of these earthquakes were performed utilizing the Carey (1979) method (Figure 9). Considering the epicenters of these earthquakes and the active faults in the region, it is concluded that the main motion planes of all three earthquakes are in the ENE-WSW direction (plane 1 values in Table 1). By contemplating the focal mechanism solutions of the earthquakes and active faults in the region (Figure 9), it can be concluded that the May and June 1986 earthquakes were generated by the Sürgü Fault, while the Ekinözü earthquake on 16.06.2013 was generated by the Çardak Fault. Based on the focal mechanism solutions of these earthquakes, it can be inferred that the source of these earthquakes are left-lateral strike-slip faults (Figure 9). Therefore, these earthquakes which were generated by the Sürgü and Çardak faults, show that the left-lateral strike-

[1]KOERI-RETMC (2021). Recent Earthquakes in Turkey [online]. Website http://www.koeri.boun.edu.tr/sismo/zeqdb/indexeng.asp [accessed 18 July 2021].

[2]Global CMT Catalogue (2021). Global CMT Catalog Search [online]. Website https://www.globalcmt.org/CMTsearch.html [accessed 18 July 2021].

[3]AFAD (2021). Afet ve Acil Durum Yönetimi Başkanlığı Deprem Dairesi Başkanlığı. Website: https://deprem.afad.gov.tr/faycozumleri?lang=en [accessed 18 July 2021].

Figure 8. Topographic elevation difference and stream offset in Barış village (looking towards SE). The yellow dashed line shows the fault line, the blue dashed lines show the offset on channel edges, and the white arrows show the elevation difference.

Table 1. Parameters of the earthquakes that were analyzed in the study area.

No	Date (dd.mm.yy)	Time (hh:mm:ss)	Lat. (°)	Lon. (°)	Plane 1 str°/dip°/rake°	Plaane 2 str°/dip°/rake°	Mag. (Mw)	Depth (km)	Reference
a1	05.05.1986	03:35:41	37.72	37.70	260/54/9	164/82/144	6.0	15	Global CMT
	05.05.1986	03:35:38	38.02	37.79	273/49/31	161/67/135	5.8	4	Taymaz et al., 1991; Tan et al., 2008
a2	06.06.1986	10:39:49	37.36	37.99	250/90/0	160/90/180	5.8	15	Global CMT
	06.06.1986	10:39:47	38.01	37.91	275/27/30	158/77/114	5.6	11	Taymaz et al., 1991; Tan et al., 2008
a3	16.06.2013	20:31:38	38.11	37.08	73/85/21	341/69/175	4.1	10	AFAD

slip faulting that developed the approximately NNE-SSW trending compressional forces are dominant in the region (Figure 9).

4. Paleoseismological trenching

Paleoseismology is a common and efficient method to obtain reliable data on the existence and past activity of active faults. In this method, depending on the purpose, evaluations are made based on sedimentology, stratigraphy and structural geology within the trenches that are dug perpendicular or parallel to the active fault trace and paleoearthquakes are dated by collecting samples from critical stratigraphic levels (McCalpin, 2009).

The carbon 14 (^{14}C) dating method, also known as the radiocarbon dating method, is one of the main dating methods in paleoseismological studies. Within the framework of this study, 6 samples from 2 trenches on the Sürgü Fault and 5 samples from 2 trenches on the Çardak Fault were collected and dated with the ^{14}C method in the laboratory of The Scientific and Technological Research Council of Türkiye-Marmara Research Center (TÜBİTAK-MAM).

In this study, Google Earth was initially used to identify possible trench sites. Then, field reconnaissance was undertaken of fault-related geomorphologic indicators and to confirm trench sites along the Sürgü and Çardak faults. As a result, four trenches were excavated: the Kurucaova and Sürgü-East trenches (Figure 10) were excavated 8-km apart on the Sürgü-1 (eastern) section of the Sürgü Fault, and the Barış-1 and Barış-2 trenches were excavated 12 m apart on the Çardak-1 (eastern) section of the Çardak Fault.

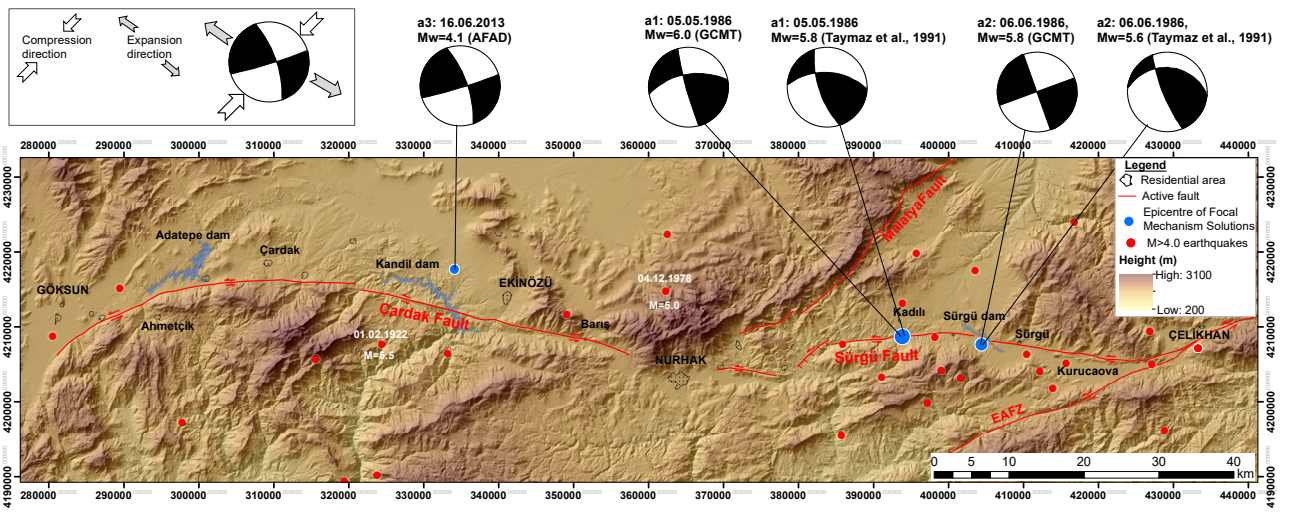

Figure 9. The epicenters and focal mechanism solutions of the 1986 Doğanşehir earthquakes and the 2013 Ekinözü earthquake with distribution of the earthquakes in the study area throughout the instrumental period (1900–2021; KOERI-RETMC, 2021) on DEM.

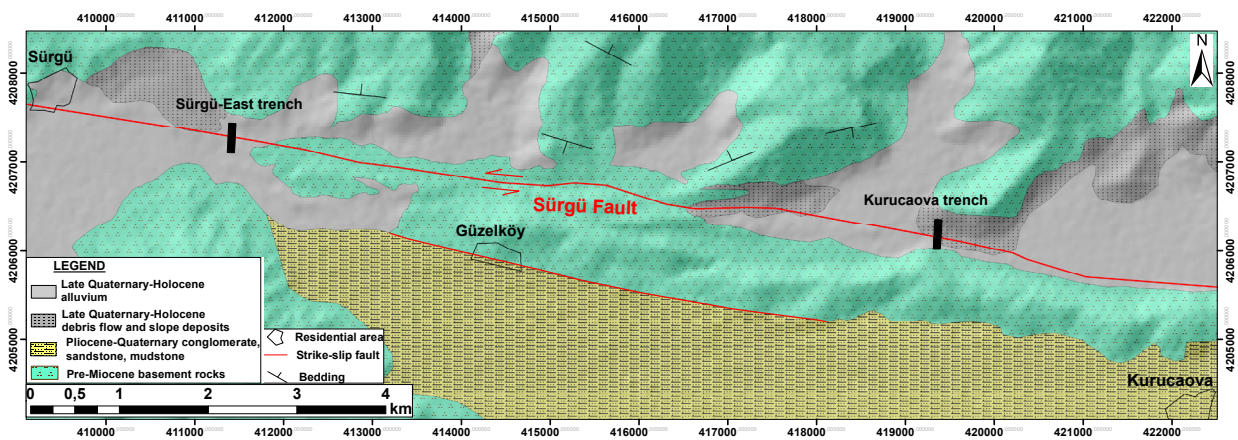

Figure 10. Trench locations in the eastern part of the Sürgü Fault.

4.1. Kurucaova trench

About 3-km NW of Kurucaova, a trench was excavated where the valley narrowed down, the groundwater level is low, the sedimentation conditions are favorable. At this point, the fault was located in a narrow 100 m wide zone. Starting from the hillslope in the north of the valley, a trench with an average depth of 2.70 m and a length of 100 m was dug towards the south (Figure 11). After cleaning the trench walls, gridding, logging and photographing were carried out from the south in the first 35 m of the trench where the fault was identified.

Fine-grained levels representing colluvium and flood plain deposits are dominant in the trench. In these sediment packets, pebble and sand lenses and interbeds reflect channel and point bar deposits (Figure 12). The greenish-brown clay unit, which is the oldest unit in the trench, is observed at the southern end of the trench (up to 9 m from the south). The inclined coarse sandy, pebbly brown clay unit is observed in the fault zone. On the northern side of the fault, the brown clay unit with little sand, which spreads at the bottom of the trench wall was determined that contains sandy silt and pebbly clay lenses sporadically. Between meters-11 and -19

Figure 11. General view of Kurucaova trench site (looking towards SW). Red arrows indicate fault.

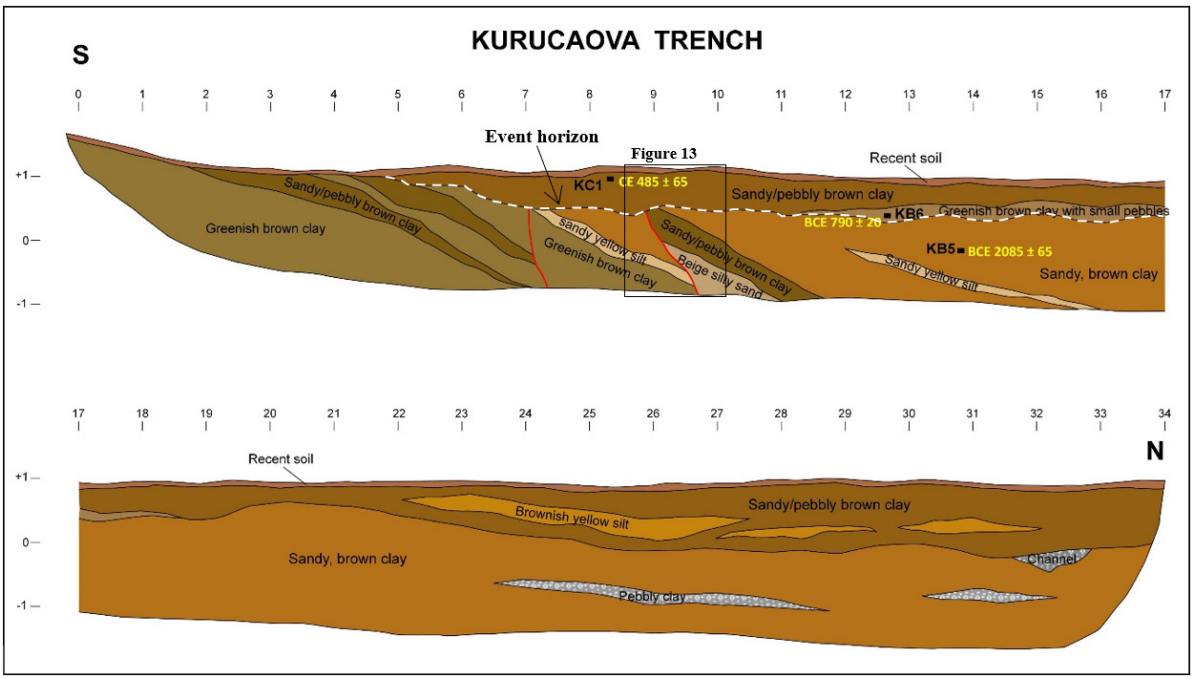

Figure 12. Log of the west wall of the Kurucaova trench (see Figure 10 for trench location).

in the trench, a 20 cm thick greenish-brown clay interlayer with small pebbles overlies the brown clay unit with little sand. Brownish-yellow silt interlayers were observed in the brown sand/clay with small pebbles, which exhibits a gradual transition with the underlying units.

Two fault strands were identified between meters-7 to -9 in the trench (Figures 12 and 13). The stratigraphic units in the faulted section are dipping towards the north. However, farther from the fault zone, it was observed that the units were essentially horizontal. In the trench, three ^{14}C samples were taken and analyzed (Table 2), two from the unit that covers the fault strands, and one from the faulted unit. Based on these dates, the age of the faulted unit is 2085 ± 65 BCE (Figure 12). Close to the fault zone, the sedimentary units are inclined as a result of the deformation and the event horizon has been truncated by erosion and later buried by younger deposits that have ages of 790 ± 20 BCE and 485 ± 65 CE. These relationships indicate at least one surface rupturing earthquake event in the Kurucaova trench. The most recent earthquake rupture occurred between 790 ± 20 BCE and 2085 ± 65 BCE. While the fault strands at meters-7 to -9 may indicate the same earthquake, it is also possible that the fault strand at meter-7 relates to an older earthquake event.

4.2. Sürgü-East trench

About 1-km east of the Sürgü village, the Sürgü-East trench was dug on an old stream bed along the Sürgü Fault. At this site, required conditions such as favorable sedimentation, low groundwater level, and effective transportation of the excavator are considered profoundly during the selection for trenching in this location. This trench, which was opened in a N-S direction, is 24 m long and 2 m deep.

In the Sürgü-East trench, brown silt and clay units containing limestone blocks and pebbles, which generally represent colluvium and fluvial deposits, were logged. The fine-grained, brown clay unit with little pebbles lies at the bottom of the trench. This sediment package is overlain by a yellow-brown clay-silt unit contains a few limestone blocks

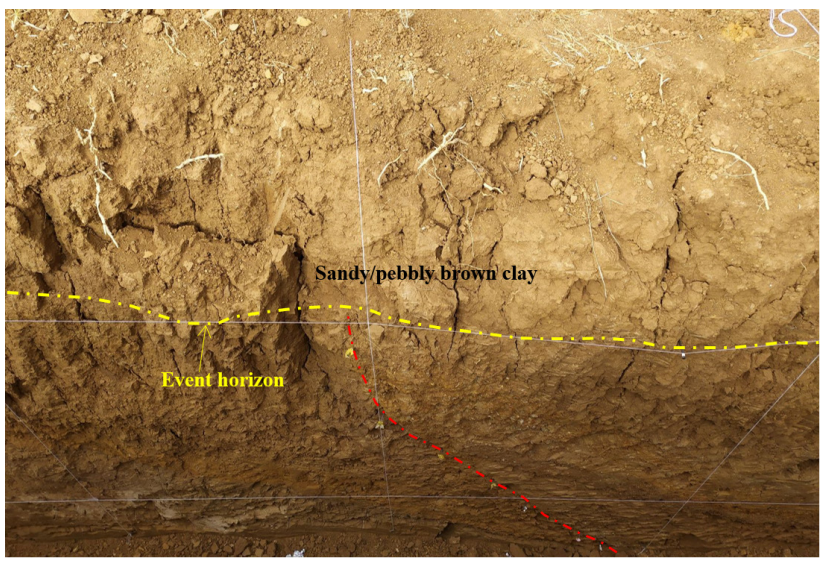

Figure 13. The fault (red dashed line) at meter-9 on the western wall of the Kurucaova trench.

Table 2. The 14_c dating results from paleoseismic sites on Sürgü Fault.

Trench site	Sample ID	Lab number	Material type	Radiocarbon age (BP)	Calibrated age (2-sigma)
Kurucaova	KC1	TÜBİTAK-1528	Charcoal	1579 ± 23	420–540 CE
Kurucaova	KB5	TÜBİTAK-1529	Bulk	3701 ± 30	2152–2018 BCE
Kurucaova	KB6	TÜBİTAK-1530	Bulk	2594 ± 24	810–771 BCE
Sürgü-East	B1	TÜBİTAK-991	Bulk	8351 ± 37	7520–7335 BCE
Sürgü-East	B2	TÜBİTAK-992	Bulk	4490 ± 31	3349–3089 BCE
Sürgü-East	B3	TÜBİTAK-993	Bulk	4596 ± 34	3383–3328 BCE

and pebbles. The dark brown clay matrix contains limestone pebbles and blocks that unconformably overlie the former unit, and it is moderately consolidated. The youngest unit in the trench is a brown clay with pebbles that contains abundant limestone clasts and a few serpentinite blocks (Figure 14).

A discontinuity which is reflecting an old earthquake event was detected in this trench (Figures 14 and 15). This discontinuity, which represents a 5–6 cm wide fissure with 15–18 cm of vertical motion along the south block is evident with the infill material. In order to evaluate the date of this event, 3 sediment samples were taken from: the infill, the unit that covers it, and the unit cut by it (Figures 14 and 15). The collected samples were sent to TÜBİTAK-MAM laboratory for ^{14}C age determination analysis (Table 2). Laboratory results indicate the age of sample B1 taken from the unit that was cut by the infill is 7430 ± 95 BCE, the age of sample B2 taken from the unit overlying the infill is 3220 ± 130 BCE, and the age of sample B3 taken from the infill itself is 3350 ± 25 BCE. Evaluation of these results and the trench logs indicate that after that earthquake, the brown clay with pebble/block was deposited and the clays filled the open fissure during this deposition. The unit that is cut by the infill is much older than the overlying and the infill unit, which indicates an erosional process. Based

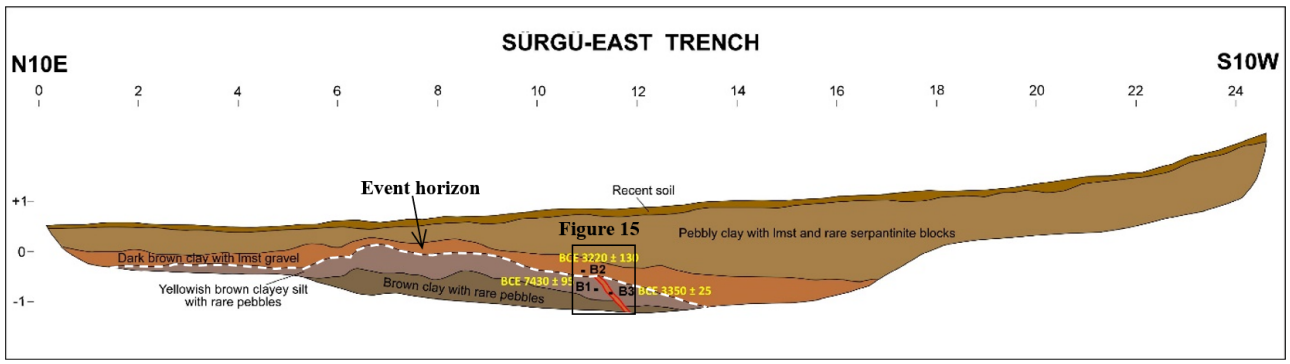

Figure 14. Log of the east wall of the Sürgü-East trench (see Figure 10 for trench location).

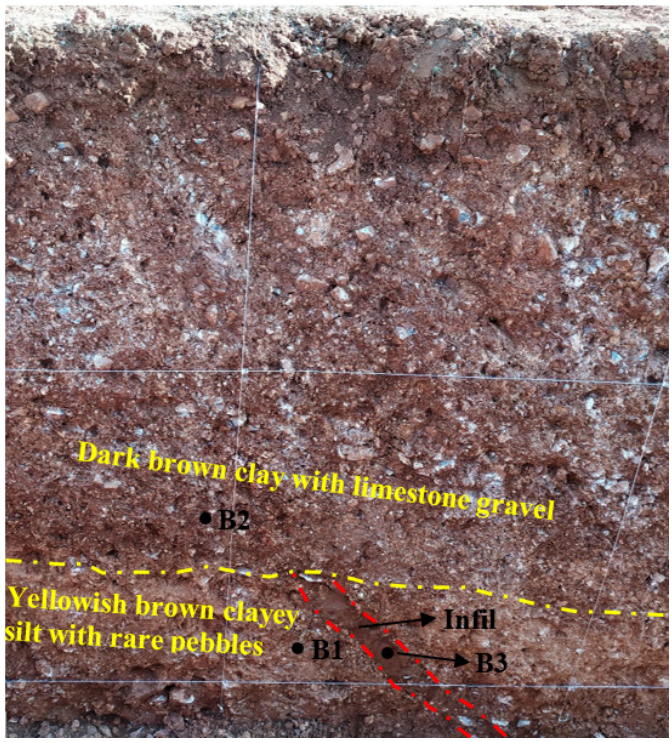

Figure 15. The view of infill on the east wall of the Sürgü-East trench and the locations of the samples.

on these relationships, the formation of the infill related to faulting, occurred around 3400 BCE, shortly before the infill and deposition process. Modeling of this event in OxCal yields an age of 3400–3340 cal year BCE (Table 2 and Figure 23).

4.3. Barış-1 trench

At 1-km west of Barış village, the Barış-1 trench was excavated across the Çardak Fault (Figure 16). This trench was excavated where there was a prominent fault scarp (Figure 17), suitable sedimentation, favorable groundwater level and easy access. A 70-m sinistrally offset stream bed is another important active fault indicator (Figure 7) at 1-km east of trench site.

The Barış-1 trench is 32 m long and up to 3 m deep. Serpentinite forms the bedrock within the trench; which is typically overlain by yellow to dark brown clay units of Late Quaternary age. Within this clay unit limestone blocks of various sizes, which are derived from the hillside at the north of the fault, and interlayers of pebble with silt-clay matrix were mapped (Figure 18). It was observed that the reddish-brown clay with pebbles that overlays the serpentinite basement rock at the bottom of the trench, generally contains caliche patches and fissures. The clay unit with pebbles, blocks, and silt that overlays the reddish-brown clay represents color patterns ranging from yellowish-brown to greenish-yellow in the trench. A gradual transition was observed between these two units (the reddish-brown clay and clay unit with pebbles, blocks, and silt). In the southern part of the trench, a sediment package consisting of coarse limestone blocks and pebbles was observed in a brown clay matrix. The youngest unit

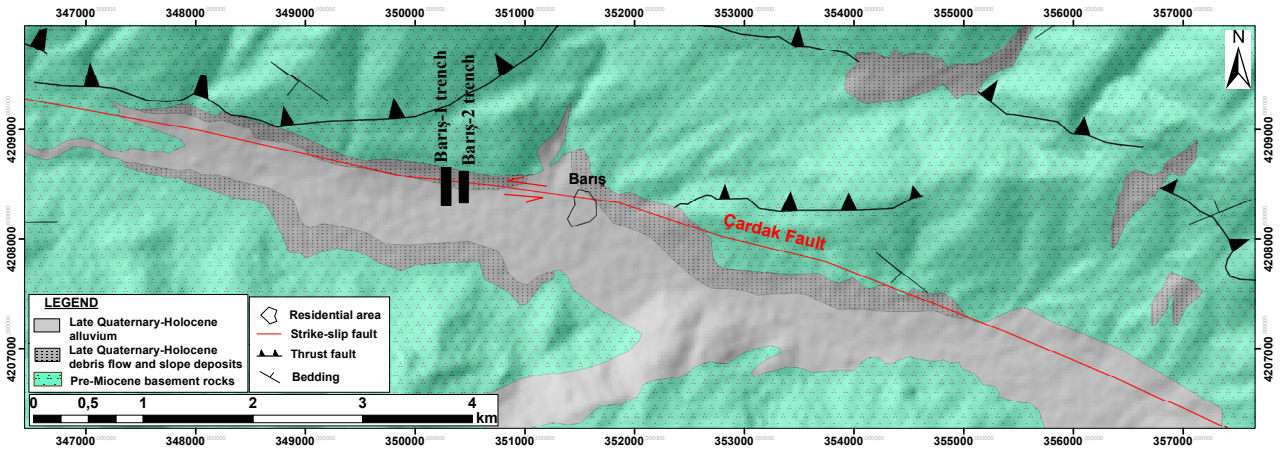

Figure 16. Location of the Barış trenches on the geological map of the eastern section of the Çardak Fault.

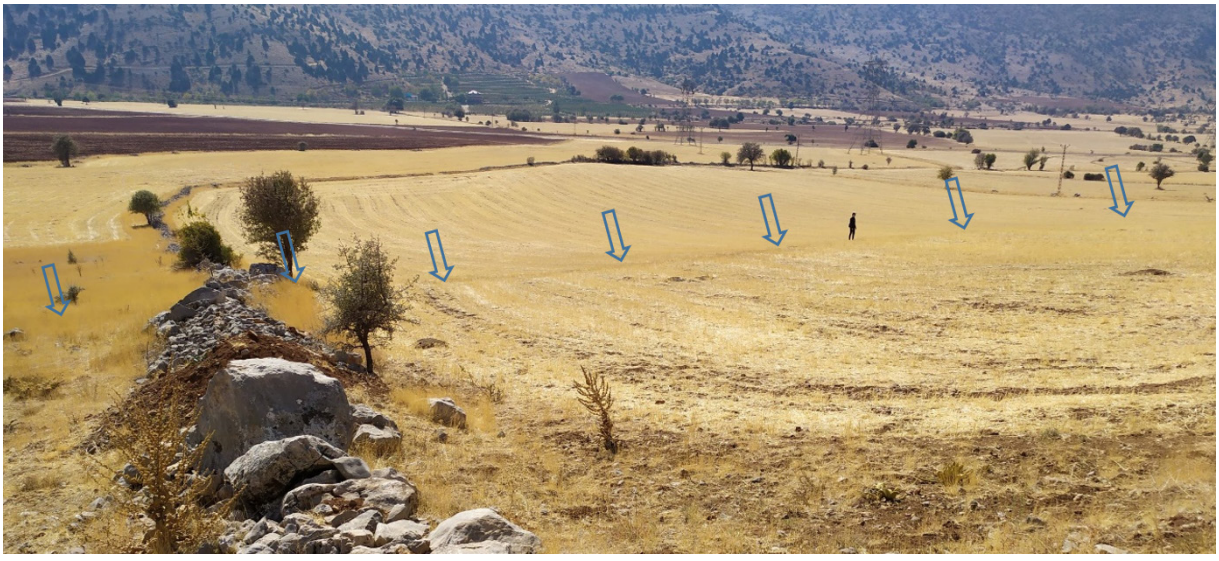

Figure 17. The fault scarp along the Çardak Fault, west of the Barış trenches (looking towards SW).

on the trench wall consists of brown clay with limestone pebbles and blocks (Figure 18).

There are two main zones of deformation in the trench. Between meters-3 and -4 in the trench, are fault strands in the bedrock related to older earthquake (Figures 18 and 19). Between meters-16 to -17 of the trench, fault strands that cut the cover unit of the old fault indicate a younger paleoearthquake rupture (Figures 18 and 20). These fault branches indicate that at least two surface-rupturing earthquakes occurred on the Çardak Fault. Radiocarbon dating results from the Barış-1 trench indicate the following: the age of the unit cut by the old fault is 10520 ± 95 BCE; the age of the unit that covers the old fault and is cut by the relatively young fault is 4950 ± 105 BCE; and, the age of another unit cut by the young fault is 3215 ± 125 BCE (Table 3). The relevance of these dates will be discussed further below.

4.4. Barış-2 trench

The Barış-2 trench was excavated with dimensions of 26 m in length and up to 3 m in depth, close to Barış-1 (Figure 16). In this trench, in addition to the units described in the Barış-1 trench, a light brown clay with limestone gravels and dark brown clay units, a brown clay with pebble interlayers and limestone blocks between the meters-4 to -9, and a brown clay lens was detected between the meters-11 to -16 were all logged in the trench walls (Figure 21).

The Barış-2 trench also exposed two zones of fault deformation that correlate well with those described

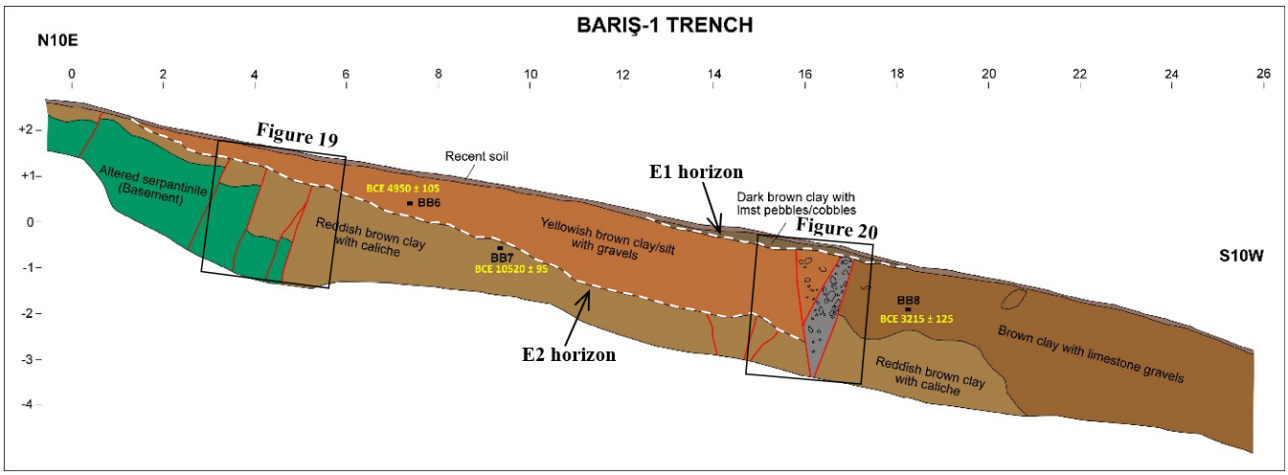

Figure 18. Log of the east wall of the Barış-1 trench (see Figure 16 for trench location).

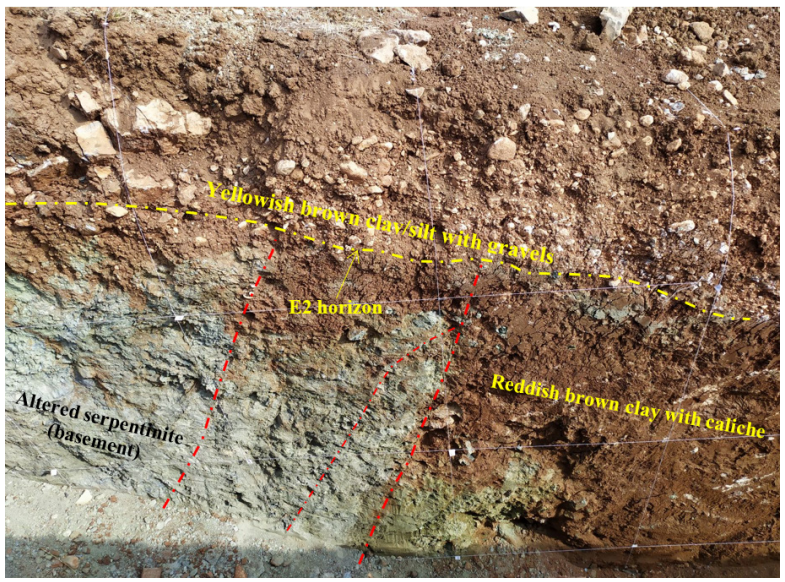

Figure 19. The traces of bedrock faults (red dashed lines) at meters-3 to -4 on the eastern wall of the Barış-1 trench.

Table 3. The ^{14}C dating results from paleoseismic sites on Çardak Fault.

Trench site	Sample ID	Lab number	Material type	Radiocarbon age (BP)	Calibrated age (2-sigma)
Barış-1	BB6	TÜBİTAK-1533	Bulk	6066 ± 37	5061–4846 BCE
Barış-1	BB7	TÜBİTAK-1534	Bulk	10476 ± 38	10613–10426 BCE
Barış-1	BB8	TÜBİTAK-1535	Bulk	4485 ± 30	3344–3089 BCE
Barış-2	BB2	TÜBİTAK-1531	Bulk	1228 ± 22	763–880 CE
Barış-2	BB4	TÜBİTAK-1532	Bulk	6893 ± 31	5844–5717 BCE

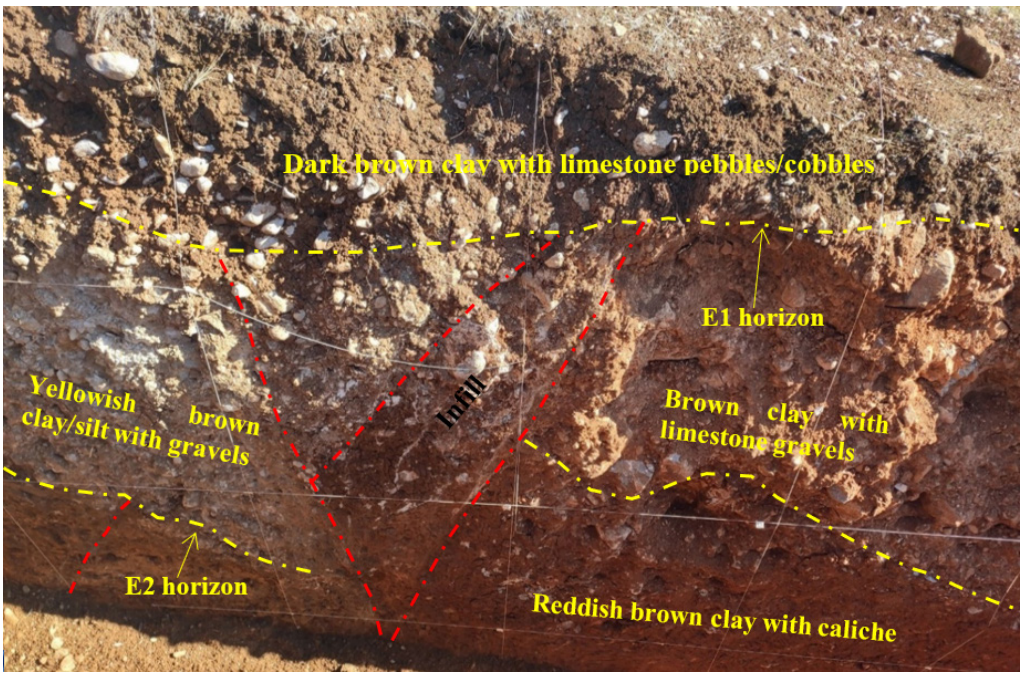

Figure 20. The fault strands (red dashed lines) between the meters-15 and -17 on the eastern wall of the Barış-1 trench.

from the Barış-1 trench. The main bedrock fault zone was displayed in the Barış-2 trench at meter-8. Significantly, the younger fault zone was clearly expressed at meter-21 displaying upward-terminating fault relationships (Figures 21 and 22). The sharp juxtaposition of units between meters-18 and -21 across these faults is indicative of strike-slip faulting.

Two ^{14}C samples were taken from units associated with this fault termination. The age of the unit cut by the relatively young fault is 5780 ± 65 BCE, and the age of the unit overlying the young fault is 825 ± 55 CE (Table 3). By combining the relationships and dating results from both the Barış-1 and Barış-2 trenches it is inferred that the Çardak Fault generated at least one earthquake between 10520 ± 95 BCE and 5780 ± 65 BCE, and one young paleoearthquake between BCE 3215 ± 125 and CE 825 ± 55.

5. Discussion and conclusion

In this study, the paleoseismological characteristics of the Sürgü and Çardak faults, which splay from the EAFZ in the south of Çelikhan were investigated. Being the first study to date the Late Holocene earthquakes on the Sürgü and Çardak faults reveals the importance of this research.

With this study, structural and morphological elements such as stream and river offsets, fault scarps, linear valleys, small depression basins, linear trough, shutter ridge, pressure ridge, faulted late Quaternary colluvium and alluvium outcrops along the Sürgü and Çardak faults were observed and analyzed. As a result of the investigations, it is concluded that the Sürgü and Çardak faults are active structures and they are predominantly controlled by left-lateral strike-slip motion.

The epicentral location of the Ekinözü earthquake that occurred on 16 June 2013 and the Doğanşehir

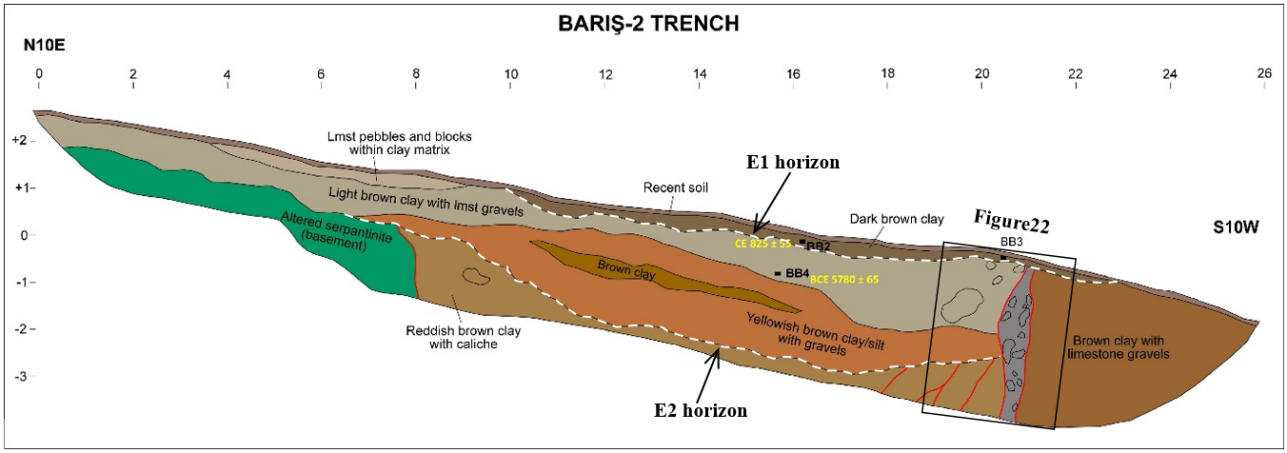

Figure 21. Log of the east wall of the Barış-2 trench (see Figure 16 for trench location).

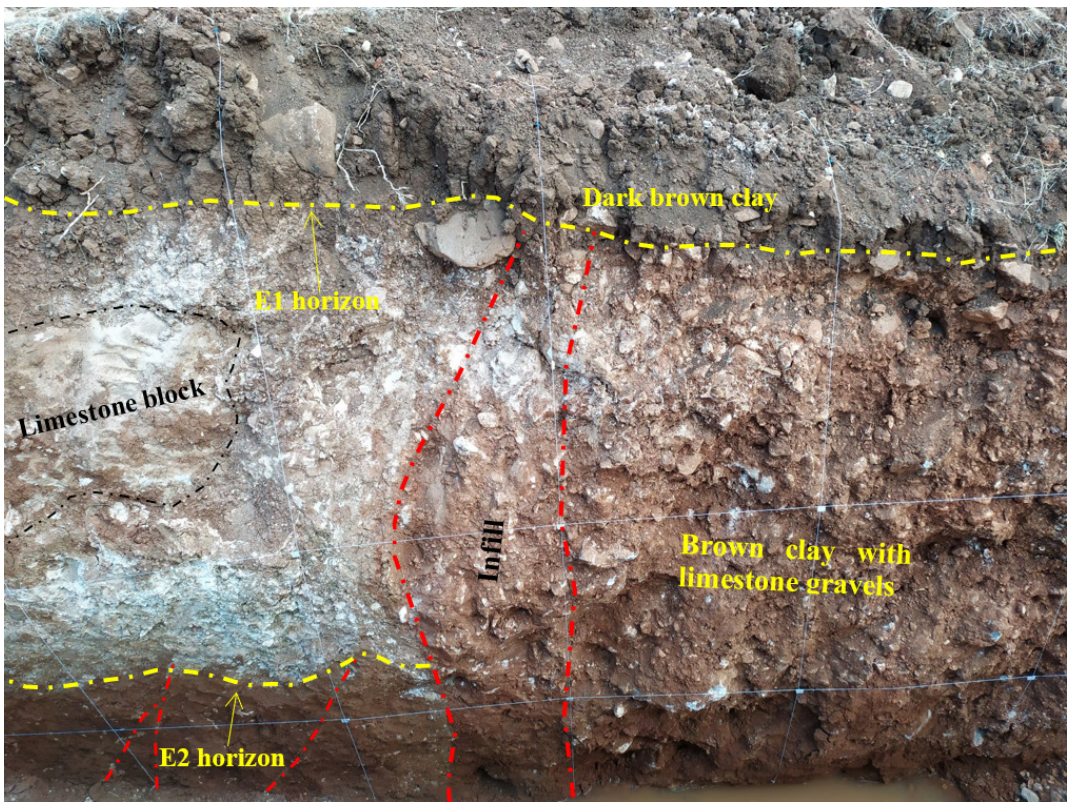

Figure 22. The fault strands between meters-18 and -21 of the eastern wall of the Barış-2 trench. The red dashed lines show the faults.

earthquakes that occurred in 5 May (M = 5.8) and 6 June (M = 5.6) 1986 and their focal mechanism solutions were examined. It is deduced that the 1986 Doğanşehir earthquakes were generated by the Sürgü Fault, and the 2013 Ekinözü earthquake was produced by the Çardak Fault. Furthermore, based on the focal mechanism solutions of these three earthquakes produced by the Sürgü and Çardak faults (Taymaz et al., 1991; Tan et al., 2008; Ekström et al., 2012; AFAD, 2021) it can be stated that the sinistral strike-slip faulting was developed by the NNE-SSW trending compression regime that is dominant in the region (Figure 9).

Duman and Emre (2013) suggested that the Sürgü Fault denote slip rates of 3 mm/year, and the Çardak Fault,

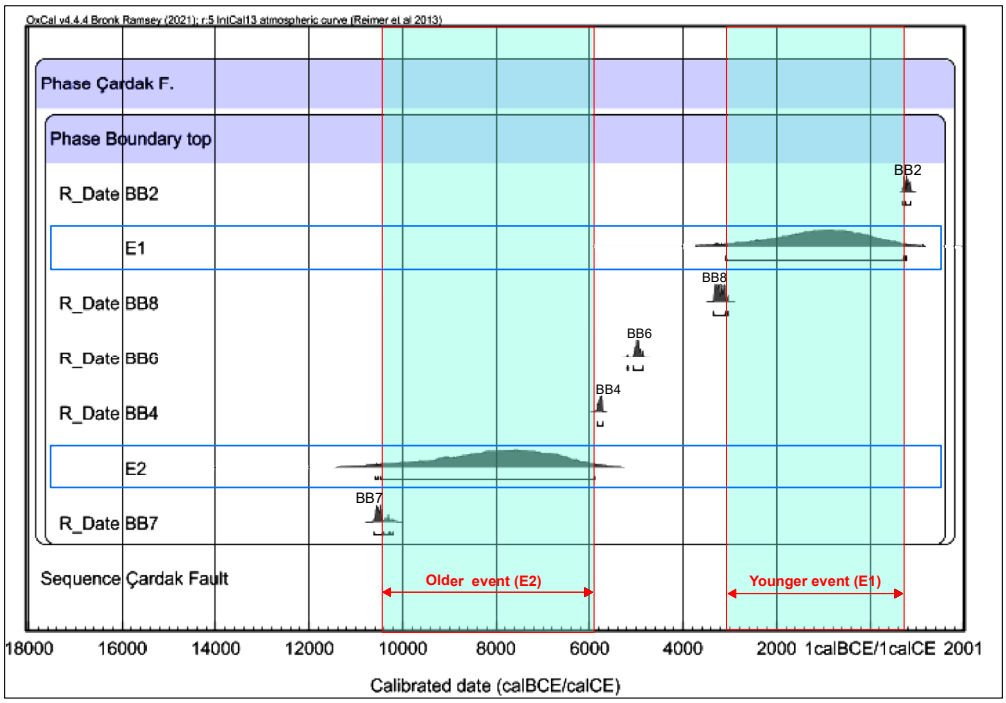

Figure 24. The graphic shows calibration of the collected samples from the Barış-1 and Barış-2 trenches using OxCal v4.4.4 and the time interval of earthquakes detected on the Çardak Fault (Bronk Ramsey, 2017; Reimer et al., 2020). BB6, BB7 and BB8 represent the sample numbers of samples taken from the Barış-1 trench, yet BB2 and BB4 indicate the sample numbers taken from Barış-2 trench.

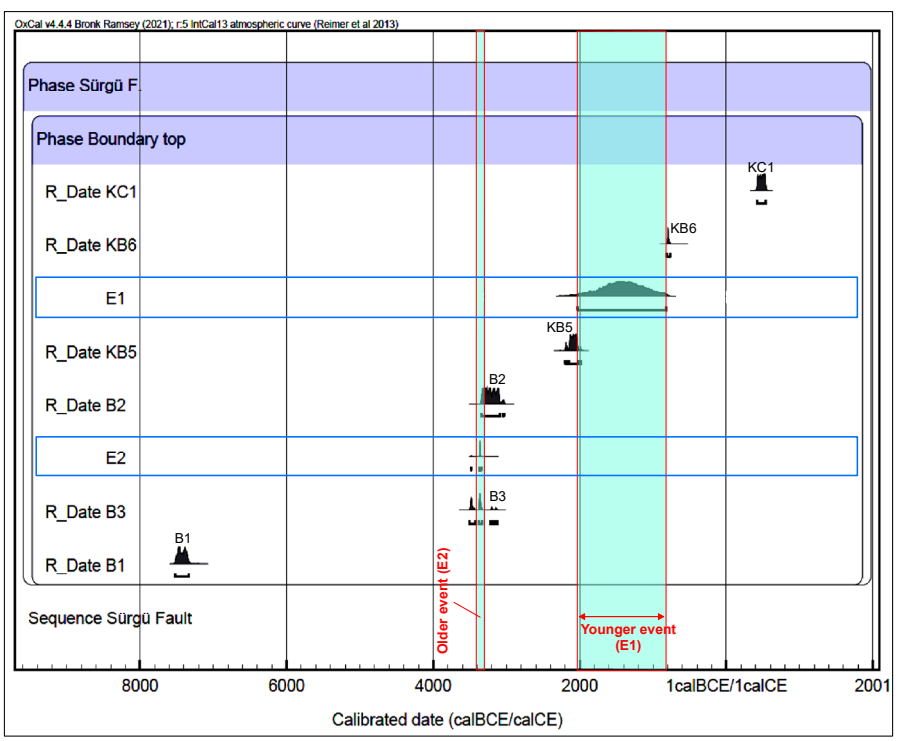

Figure 23. The graphic shows calibration of the collected samples from the Sürgü-East and Kurucaova trenches using OxCal v4.4.4 and the time interval of earthquakes detected on the Sürgü Fault (Bronk Ramsey, 2017; Reimer et al., 2020). KC1, KB5 and KB6 represent the sample numbers of samples taken from the Kurucaova trench, yet B1, B2 and B3 indicate the sample numbers taken from Sürgü-East trench.

2.5 mm/year. According to these data, a slip of 3 m on the Sürgü Fault and 2.5 m on the Çardak Fault accumulates during 1000 years. This data showing to importance of a revealing seismic hazards of the Sürgü and Çardak Faults.

Four trenches were excavated on the Sürgü and Çardak faults within the scope of paleoseismological studies. Eleven samples were taken from the four trenches and dated using the radiocarbon method (Tables 2 and 3). The results calibrated by using OxCal v4.4.4 (Bronk-Ramsay 2009, 2017). In order to reveal the earthquake history of the faults, trench studies and laboratory results were evaluated meticulously for each fault separately. Based on the results from the two trenches on the Sürgü Fault, it is concluded that the Sürgü Fault generated at least two Late Holocene earthquakes: one around 3400 BCE, and one between 2085 ± 65 BCE and 790 ± 20 BCE (Figure 23). Other results from the two trenches near Barış indicate that the Çardak Fault produced at least one earthquake between 10520 ± 95 BCE and 5780 ± 65 BCE, and one earthquake event that created a surface rupture between 3215 ± 125 BCE and 825 ± 55 CE (Figure 24). The last earthquake may be correlated with the 584/587 CE earthquake (Guidoboni et al., 1994; Ambraseys, 2009) that caused extensive destruction in Elbistan, but it is also possible an older one due to large time span for the last earthquake.

Pondering the paleoseismological data and findings associated with the Sürgü and Çardak faults it is deduced that the time span of earthquakes on the Sürgü Fault and the Çardak Fault are inconsistent with each other (Figures 23 and 24). Moreover, the Nurhak Fault Complex between the Sürgü and Çardak faults likely constitutes a structural barrier in terms of seismic segment behavior. Because of these, the seismic history of the Sürgü and Çardak faults is different and they have not been ruptured together in the past.

By the historical and instrumental earthquake data of the Sürgü and Çardak faults, and based on their segment lengths (e.g., Wells and Coppersmith, 1994), it has been concluded that each of these faults has the potential to produce earthquakes with minimum magnitude 7.

While the evaluation process of this article was continuing, 6 February 2023 earthquakes occurred. As a result of the field studies conducted by two of the authors in the earthquake region immediately after the earthquakes, it was observed that a 100-km long surface rupture occurred on the Çardak Fault in the Ekinözü earthquake (13.24; Mw 7.6). It was observed that the Barış-1 and Barış-2 trenches, which were dug during the paleoseismological studies on the Çardak Fault within the scope of this article, were clearly offset to the left (Supplementary Figures a and b). In this earthquake, a 5.4 ± 0.3 m offset at the field boundary just west of the Barış-1 trench and 6.5 ± 0.25 m in a small channel 80 m east of the Barış-2 trench was detected (Supplementary Figure c).

Acknowledgment

This study constitutes a part of Musa Balkaya's doctoral thesis. The study was supported by Çanakkale Onsekiz Mart University Scientific Research Projects Coordination Unit (FDK-2019-2979) and TÜBİTAK-1002 Quick Support Projects (120Y102). We are grateful to ÇOMÜ-BAP and TÜBİTAK for their financial supports. We would like to thank Mehran Basmenji for help in English translation. We would also like to thank the editor and anonymous reviewers for their valuable comments and suggestions, which improved the quality of the manuscript.

References

Allen CR (1969). Active faulting in northern Turkey, Contr.1577. Division of Geology Sciences. California Institute of Technology 32s.

Ambraseys N (2009). Earthquakes in the Mediterranean and Middle East: a multidisciplinary study of seismicity up to 1900. Cambridge University Press.

Arpat E, Şaroğlu F (1972). Doğu Anadolu Fayı ile ilgili bazı gözlemler ve düşünceler. MTA Dergisi 78: 44-50 (in Turkish).

Arpat E, Şaroğlu F (1975). Türkiye'deki bazı önemli genç tektonik olaylar. Türkiye Jeoloji Kurumu Bülteni 18 (1): 91-101 (in Turkish).

Balkaya M, Özden S, Akyüz HS (2021). Morphometric and Morphotectonic characteristics of Sürgü and Çardak Faults (East Anatolian Fault Zone). Journal of Advanced Research in Natural and Applied Sciences 7 (3): 375-392. https://doi.org/10.28979/jarnas.939075

Balkaya M (2022). Sürgü ve Çardak Faylarının (Doğu Anadolu Fay Zonu) Morfotektonik ve Paleosismolojik Özellikleri. PhD, Çanakkale Onsekiz Mart University, Çanakkale, Turkey (in Turkish).

Barka A, Reilinger R (1997). Active tectonics of the Eastern Mediterranean region: deduced from GPS, neotectonic and seismicity data. Annali di Geophis. XI 587–610.

Bedi Y, Yusufoğlu H (2018). 1/100.000 ölçekli Türkiye Jeoloji Haritaları, Malatya-L40 paftası. no: 261, Maden Tetkik ve Arama Genel Müdürlüğü, Ankara (in Turkish).

Bronk Ramsey C (2017). Methods for summarizing radiocarbon datasets. Radiocarbon 59 (6): 1809-1833.

Carey E (1979). Recherche des directions principales de contraintes associées au jeu d'une population de failles. Revue de Géologie Dynamique et de Géographie Physique 21 (1): (in French).

Çoban M, Dalkılıç H (2018). 1/100.000 ölçekli Türkiye Jeoloji Haritaları, Şanlıurfa-M39 paftası. no: 262, Maden Tetkik ve Arama Genel Müdürlüğü, Ankara (in Turkish).

Dewey JF, Hempton MR, Kidd WSF, Şaroğlu F, Şengör AMC (1986). Shortening of continental lithosphere: the neotectonics of Eastern Anatolia a young collision zone. Geology Society London, Special Publication 19: 3-36 s.

Duman TY, Emre O (2013). The East Anatolian fault: geometry, segmentation and jog characteristics. Geological Society Publications 372: 495–529. https://doi.org/10.1144/SP372.14

Ekström G, Nettles M, Dziewonski AM (2012). The Global CMT project 2004-2010: centroid-moment tensors for 13,017 earthquakes. Physics of the Earth Planetary Interiors 200-201: 1-9. https://doi.org/10.1016/j.pepi.2012.04.002

Emre Ö, Duman TY, Özalp S, Elmacı H, Olgun Ş et al. (2013). Active fault map of Turkey with an explanatory text 1:1,250,000 scale. General Directorate of Mineral Researchand Exploration, Special Publication Series 30.

Emre Ö, Duman TY, Özalp S, Şaroğlu F, Olgun Ş et al. (2016). Active fault database of Turkey. Bulletin of Earthquake Engineering 1-47. https://doi.org/10.1007/s10518-016-0041-2

Guidoboni E, Comastri A, Traina G, Rom Istituto Nazionale di Geofisica. (1994). Catalogue of Ancient Earthquakes in the Mediterranean Area up to the 10th Century (p. 504). Rome: Istituto nazionale di geofisica.

Guidoboni E, Comastri A (2005). Catalogue of Earthquakes and Tsunamis in the Mediterranean Area from the 11th to the 15th Century (p. 1037). Rome, Italy: Istituto nazionale di geofisica e vulcanologia.

Gülerce Z, Tanvir Shah S, Menekşe A, Arda Özacar A, Kaymakci N et al. (2017). Probabilistic seismic-hazard assessment for East Anatolian fault zone using planar fault source models. Bulletin of the Seismological Society of America 107 (5): 2353-2366. https://doi.org/10.1785/0120170009

Güvercin SE, Karabulut H, Konca AÖ, Doğan U, Ergintav S (2022). Active seismotectonics of the East Anatolian Fault. Geophysical Journal International 230 (1): 50-69. https://doi.org/10.1093/gji/ggac045

Herece E (2008). Doğu Anadolu Fayı (DAF) Atlası. General Directorate of Mineral Research and Exploration. Special Publications, Ankara, Serial Number 13: 359.

Koç A (2005). Remote Sensing Study of Sürgü Fault Zone (Malatya, Turkey). Master Thesis (Unpublished), Ankara.

Koç A, Kaymakci N (2013). Kinematics of Sürgü Fault Zone (Malatya, Turkey): A remote sensing study. Journal of Geodynamics 65: 292-307. https://doi.org/10.1016/j.jog.2012.08.001

Korkmaz H, Karabulut M, Gürbüz M (2008). Göksun'da Yerel Zemin Özellikleri İle Deprem Etkisi Arasındaki İlişki. 100. Yılında Göksun Sempozyumu, Kahramanmaraş.

McCalpin JP (Ed.) (2009). Paleoseismology (Vol. 95). Academic press, Amsterdam.

McClusky S, Balassanian S, Barka A, Demir C, Ergintav S et al. (2000). Global Positioning System constraints on plate kinematics and dynamics in the eastern Mediterranean and Caucasus. Journal of Geophysical Research: Solid Earth 105 (B3): 5695-5719. https://doi.org/10.1029/1999JB900351

Perinçek D, Kozlu H (1984). Stratigraphy and Structural Relations of the Units in the Afşin - Elbistan -Doğanşehir Region (EasternTauros). In: Geology of TaurosBelt (eds., O. Tekeli and M.C. Göncüoğlu). MTA, p.181-198.

Perinçek D, Günay Y, Kozlu H (1987). Doğu ve Güneydoğu Anadolu Bölgesindeki Yanal Atımlı Faylar İle İlgili Yeni Gözlemler, Türkiye 7. Petrol Kongresi 89-103 (in Turkish).

Reilinger R, McClusky S, Vernant P, Lawrence S, Ergintav S et al. (2006). GPS constraints on continental deformation in the Africa-Arabia-Eurasia continental collision zone and implications for the dynamics of plate interactions. Journal of Geophysical Research: Solid Earth 111 (B5). https://doi.org/10.1029/2005JB004051

Reimer PJ, Austin WE, Bard E, Bayliss A, Blackwell PG et al. (2020). The IntCal20 Northern Hemisphere radiocarbon age calibration curve (0–55 cal kBP). Radiocarbon, 62 (4): 725-757.

Sunkar M, Günek H, Canpolat C (2008). Kurucaova ve Yakın Çevresinin (Malatya) Jeomorfolojisi. Fırat Üniversitesi Sosyal Bilimler Dergisi Cilt, Elazığ 18: 2: 1-22 (in Turkish).

Sümengen M (2014a). 1/100.000 ölçekli Türkiye Jeoloji Haritaları, Gaziantep-M37 paftası. no: 215, Maden Tetkik ve Arama Genel Müdürlüğü, Ankara (in Turkish).

Sümengen M (2014b). 1/100.000 ölçekli Türkiye Jeoloji Haritaları, Gaziantep-M38 paftası. no: 216, Maden Tetkik ve Arama Genel Müdürlüğü, Ankara (in Turkish).

Şaroğlu F, Emre Ö, Boray A (1987). Türkiye'nin Diri Fayları ve Depremsellikleri. MTA Genel Müdürlüğü, Rapor no: 8174, 394 s., Ankara (in Turkish).

Şaroğlu F, Emre O, Kuşçu I (1992). The East Anatolian Fault Zone of Turkey. Annalae Tectonicae 6: 99–125.

Şengör AC, Yilmaz Y (1981). Tethyan evolution of Turkey: a plate tectonic approach. Tectonophysics 75 (3-4): 181-241.

Tan O, Tapirdamaz MC, Yörük A (2008). The earthquake catalogues for Turkey. Turkish Journal of Earth Sciences 17 (2): 405-418.

Taymaz T, Eyidoğan H, Jackson J (1991). Source Parameters of Large Earthquakes in the East Anatolian Fault Zone (Turkey). Geophysical Journal International 106: 537–550. https://doi.org/10.1111/j.1365-246X.1991.tb06328.x

Usta D, Ateş Ş, Çoban M, Deveci Ö, Ekmekyapar A et al. (2018). 1/100.000 ölçekli Türkiye Jeoloji Haritaları, Şanlıurfa-M40 paftası. no: 263, Maden Tetkik ve Arama Genel Müdürlüğü, Ankara (in Turkish).

Wells DL, Coppersmith KJ (1994). New empirical relationships among magnitude, rupture length, rupture width, rupture area, and surface displacement. Bulletin of the seismological Society of America 84 (4): 974-1002.

Westaway R (2004). Kinematic Consistency between the Dead Sea Fault Zone and The Neogene and Quaternary Left-Lateral Faulting in SE Turkey. Tectonophysics 391: 203–237. https://doi.org/10.1016/j.tecto.2004.07.014

Yılmaz H (2002). Sürgü Fayının Neotektonik Özellikleri. Cumhuriyet Üniv. Müh. Fak. Dergisi, Seri A-Yerbilimleri, Sivas 19 (5): 35-46 (in Turkish).

Yilmaz H, Over S, Ozden S (2006). Kinematics of the East Anatolian Fault Zone Between Turkoglu (Kahramanmaras) and Çelikhan (Adıyaman), Eastern Turkey. Earth Planets and Space 58 (11): 1463-1473.

Yönlü Ö, Altunel E, Karabacak V, Akyüz HS (2013). Evolution of the Gölbaşı basin and its implications for the long-term offset on the East Anatolian Fault Zone, Turkey. Journal of Geodynamics 65: 272-281. https://doi.org/10.1016/j.jog.2012.04.013

Supplementary materials

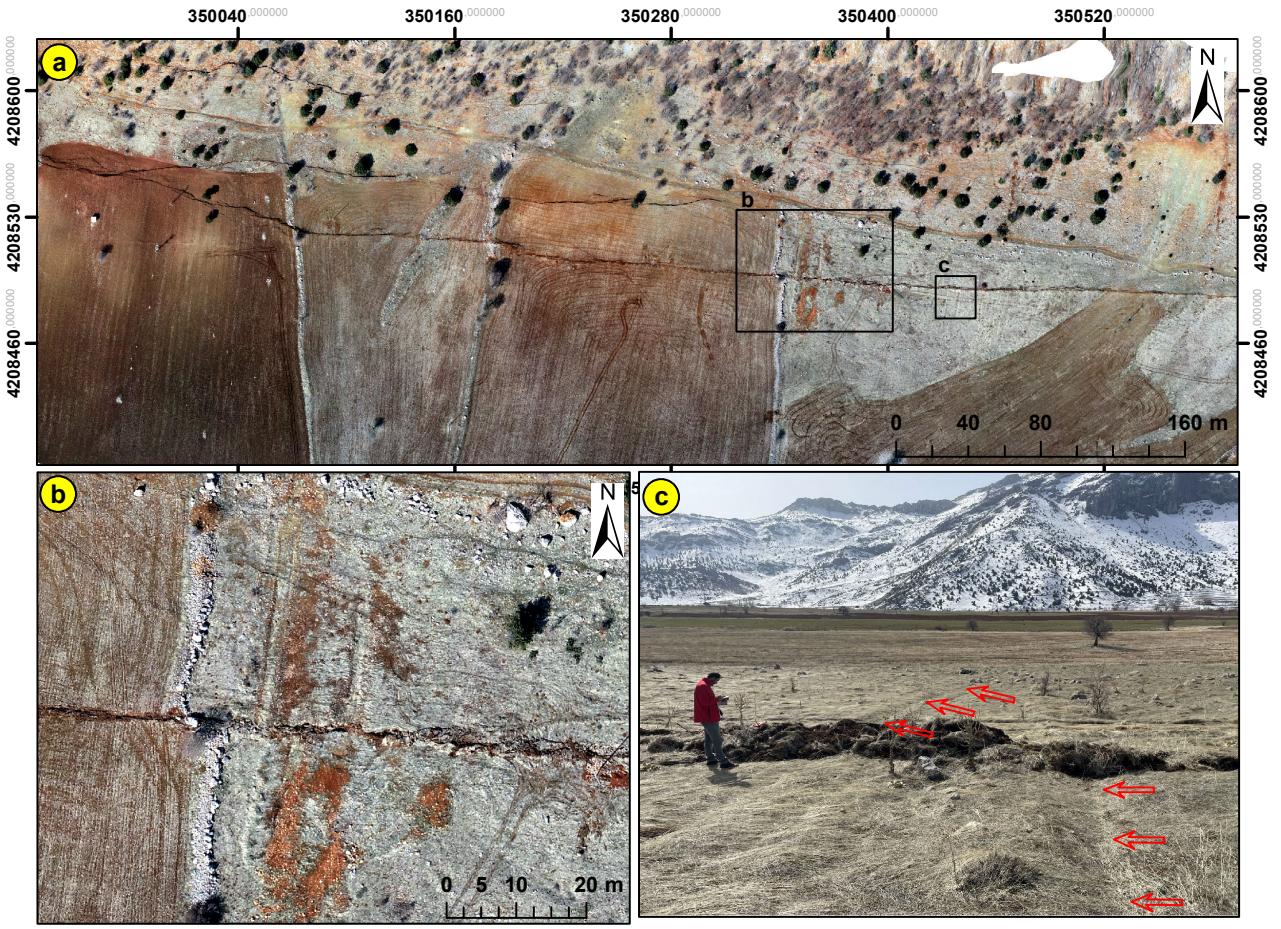

Supplementary Figure. a) The trace of the surface rupture formed after the 6 February 2023 earthquake in the west of Barış village; b) Trace of the surface rupture that offset the Barış trench and the adjacent field border by 5.4 ± 0.30 m left-laterally; c) 6.5 ± 0.25 m offset in a small channel at 80 m east of the Barış trenches (looking towards south). Red arrows show offset at the small channel.